IEEE Access
Multidisciplinary | Rapid Review | Open Access Journal

Received February 10, 2020, accepted February 24, 2020, date of publication February 27, 2020, date of current version March 12, 2020.

*Digital Object Identifier 10.1109/ACCESS.2020.2976768*

# Grid-Connected Harmonic Current Suppression of Permanent Magnet Direct Drive Wind Power Converter Based on Current Cross-Coupling Control

**ZHAOYAN ZHANG AND PEIGUANG WANG**
College of Electronic Information Engineering, Hebei University, Baoding 071002, China

Corresponding author: Peiguang Wang (pgwang@hbu.edu.cn)

This work was supported in part by the National Natural Science Foundation of China under Grant 11771115 and Grant 11271106, in part by the Hebei Province Basic Research Program Project of China under Grant F2019201095, and in part by the Hebei Talent Engineering Training Support Project under Grant A201901026.

**ABSTRACT** Due to the power-grid low-order harmonic voltage and the nonlinearity of power electronic devices, the grid-connected converter of wind power generation system produces grid-connected harmonic current. In order to improve the output power quality of full-power grid-connected converter of wind power generation system, based on the detailed analysis of the harmonic mathematical model of grid-side converter, a cross-coupling control strategy for suppressing the low-order harmonic current components is proposed in this paper. In this control strategy, the DC component of each grid-connected harmonic current is detected in the multi-synchronous rotating coordinate system, and the current cross-coupling control method is adopted to realize the accurate control of each harmonic current. The harmonic current cross-coupling controller is analyzed and designed in detail. The proposed control strategy takes into account the cross-coupling effect of each harmonic current, which can effectively reduce the interaction between each harmonic current and the fundamental current, and improve the stability of the system. Simulation and experimental test verify the correctness and feasibility of the proposed control strategy.

**INDEX TERMS** Wind power generation system, grid-connected converter, power quality, harmonic current, cross-coupling.

## I. INTRODUCTION

A kind of green energy, wind energy has been developed rapidly in the field of renewable energy sources in recent years [1]. With the increasing proportion of wind power installed capacity in the whole power system, the impact of wind power quality on power grid has been paid more and more attention [2], [3]. At present, with the new power grid operation guidelines putting forward higher and higher requirements for the low voltage ride through operation capability of wind power generation system [4]–[7], more and more attention has been paid to the wind power generation system with full power converter, which gradually entered into industrial application [8]–[13]. The wind energy resources in China are mainly concentrated in remote areas. And the connection between the wind farm and the main power grid is weak, so the bus voltage quality of the wind farm is not ideal, which is rich in low-order voltage harmonics. On the other hand, the inductance of the grid-side inlet reactor is generally small, and its working switching frequency is low, which will lead to a large degree of low-order harmonic current in the grid-connected converter. This will worsen the output power quality of the wind power generation system. Therefore, further research on the current harmonic suppression method of full-power converter for wind power generation system has important practical significance for improving the power quality of wind power generation system and improving the stability of power grid operation.

At present, the current harmonic suppression of wind power generation system has been studied in references [14]–[21]. In reference [15], a traditional PI regulator

The associate editor coordinating the review of this manuscript and approving it for publication was Qiu ye Sun.

plus multi-frequency resonance(PI-MFR) regulator is proposed for doubly-fed induction wind power generation system, and the accurate control of generator positive and negative sequence current and 5th and 7th harmonic current under unbalanced voltage is realized. In reference [17], the generation mechanism of harmonic current of permanent magnet direct drive synchronous wind generator is discussed, and the control scheme of suppressing harmonic current of permanent magnet direct drive synchronous wind generator is studied. However, the harmonic current suppression measures of grid-connected converters have not been considered in the literature. In reference [18], a grid-side converter control strategy using quasi-proportional resonance(quasi-PR) controller is proposed, which can suppress the negative sequence component and low harmonic current component of grid-connected current in permanent magnet direct drive wind power system. Because the resistance of the grid-side inlet reactor is generally very small, the influence of the grid-side low-order harmonic voltage will play a leading role in the grid-connected harmonic current suppression. In the control scheme proposed in the literature, the cross-coupling effect of harmonic current has not been considered, which will not be conducive to the accurate control of grid-connected harmonic current and ensure the stable operation of the system. On the other hand, in the scheme of using proportional resonance controller to suppress current harmonics, multiple proportional resonance controllers should be used to suppress each low harmonic current. This will cause the order of the harmonic current controller to increase sharply, which makes the parameter design of the whole control system very complex and greatly increases the difficulty of the design of the system controller.

When the power-grid voltage contains low-order harmonic voltage components (considering 5th, 7th, 11th and 13th), if the grid side converter is controlled only according to the fundamental component control mode, then the grid-side converter can not provide the appropriate harmonic compensation control voltage, and the corresponding low-order harmonic current will appear in the grid-side current. However, because the switching frequency of the grid-side converter is low and the inductance of the inlet reactor is small, its suppression effect on the low-order control voltage harmonic output of the converter is limited, which will also cause a large degree of low-order harmonic current in the grid-side current. Therefore, it is necessary to take certain measures to supress or eliminate the low-order harmonic current and improve the grid-connected power quality of wind power generation system. Based on the analysis of the harmonic model of full power converter for wind power generation system, a grid-side converter control strategy using cross-coupling control to suppress low-order harmonic current components is proposed in this paper. The harmonic current cross-coupling controller is analyzed and designed in detail. The correctness and feasibility of the proposed control strategy are verified by simulation and experiments.

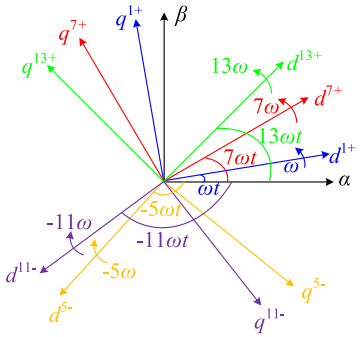


**FIGURE 1.** Multiple synchronous rotating reference coordinate.

The proposed control strategy takes into account the cross-coupling effect of each harmonic current, which can realize the accurate control of grid-connected harmonic current. And the proposed control strategy can suppress the grid-connected harmonic current caused by the power-grid low-order harmonic voltage and the nonlinear characteristics of the grid-connected converter at the same time. The proposed control strategy is of great significance to further improve the output power quality of the grid-connected full-power converter of wind power generation system.

## II. HARMONIC MODEL OF GRID SIDE INVERTER

In the three-phase static coordinate system, the rotation direction of the 5th and 11th harmonic vector is opposite to that of the fundamental vector, and the rotational electric angular velocity is $-5\omega$ and $-11\omega$, respectively. The rotation direction of the 7th and 13th harmonic vectors is the same as that of the fundamental vector, and the rotational electric angular velocity is $7\omega$ and $13\omega$, respectively. In order to reduce the interaction between harmonics and fundamental currents, and to realize the accurate control of grid-connected harmonic currents, a multi-synchronous rotating reference coordinate is established, as shown in Fig. 1.

As shown in Fig. 1, $\alpha/\beta$ coordinate is a two-phase static coordinate, and dq coordinate is a two-phase synchronous rotating coordinate. $+/-$ in the superscript represents the forward or reverse synchronous rotating coordinate respectively, and 1, 5, 7, 11 and 13 in the superscript represent the fundamental wave, 5th, 7th, 11th and 13th synchronous rotating coordinate, respectively.

In this paper, 1, 5, 7, 11 and 13 in the subscript of all equations represent fundamental wave, 5th, 7th, 11th and 13th harmonic vector or component, respectively. And the *grid* and *ctrl* in the subscript of all equations represent the grid-side electrical parameters and the control voltage component, respectively. The $d$ and $q$ in the subscript of all equations represent the synchronous rotation d and q axis components respectively, and the $a$, $b$ and $c$ in the subscript represent a phase, b phase and c phase components, respectively.

In the static three-phase coordinate system, each harmonic voltage equation of the grid-side converter can be expressed

as follows:

$$u_{abc\_k} = u_{ctrl\_abc\_k} + R_{grid} i_{abc\_k} + L_{grid} \frac{di_{abc\_k}}{dt} \quad (1)$$

In which $R_{grid}$ is the resistance of the inlet reactor, $L_{\text{grid}}$ is the inductance of the inlet reactor. $k$ is the harmonic order. $u_{abc\_k}$ is the power grid voltage harmonic vector. $u_{ctrl\_abc\_k}$ is the control voltage harmonic vector, which is generated by the controller. And $i_{abc\_k}$ is the current harmonic vector.

In the three-phase static coordinate system, the voltage equation of the grid-side converter with harmonic components is as follows:

$$u_{grid} = u_{ctrl} + R_{grid} i_{grid} + L_{grid} \frac{di_{grid}}{dt} \quad (2)$$

In which $u_{grid}$, $u_{ctrl}$, $i_{grid}$ is as follows, respectively.

$$\begin{aligned} u_{grid} = {} & u_{dq\_1}^{1+} e^{j\omega t} + u_{dq\_5}^{5-} e^{-j5\omega t} + u_{dq\_7}^{7+} e^{j7\omega t} \\ & + u_{dq\_11}^{11-} e^{-j11\omega t} + u_{dq\_13}^{13+} e^{j13\omega t} \end{aligned} \quad (3)$$

$$\begin{aligned} u_{ctrl} = {} & u_{ctrl\_dq\_1}^{1+} e^{j\omega t} + u_{ctrl\_dq\_5}^{5-} e^{-j5\omega t} + u_{ctrl\_dq\_7}^{7+} e^{j7\omega t} \\ & + u_{ctrl\_dq\_11}^{11-} e^{-j11\omega t} + u_{ctrl\_dq\_13}^{13+} e^{j13\omega t} \end{aligned} \quad (4)$$

$$\begin{aligned} i_{grid} = {} & i_{dq\_1}^{1+} e^{j\omega t} + i_{dq\_5}^{5-} e^{-j5\omega t} + i_{dq\_7}^{7+} e^{j7\omega t} \\ & + i_{dq\_11}^{11-} e^{-j11\omega t} + i_{dq\_13}^{13+} e^{j13\omega t} \end{aligned} \quad (5)$$

Equation (2) is transformed into the $dq$ synchronous rotating coordinate system by constant amplitude coordinates transformation [22]–[25].

$$\begin{aligned} u_{grid\_dq} = {} & u_{ctrl\_dq} + R_{grid} i_{grid\_dq} \\ & + L_{grid} \frac{di_{grid\_dq}}{dt} + j\omega L_{grid} i_{grid\_dq} \end{aligned} \quad (6)$$

In which $u_{grid\_dq}$, $u_{ctrl\_dq}$, $i_{grid\_dq}$ is as follows, respectively.

$$\begin{aligned} u_{grid\_dq} = {} & u_{dq\_1}^{1+} + u_{dq\_5}^{5-} e^{-j6\omega t} + u_{dq\_7}^{7+} e^{j6\omega t} \\ & + u_{dq\_11}^{11-} e^{-j12\omega t} + u_{dq\_13}^{13+} e^{j12\omega t} \end{aligned} \quad (7)$$

$$\begin{aligned} u_{ctrl\_dq} = {} & u_{ctrl\_dq\_1}^{1+} + u_{ctrl\_dq\_5}^{5-} e^{-j6\omega t} + u_{ctrl\_dq\_7}^{7+} e^{j6\omega t} \\ & + u_{ctrl\_dq\_11}^{11-} e^{-j12\omega t} + u_{ctrl\_dq\_13}^{13+} e^{j12\omega t} \end{aligned} \quad (8)$$

$$\begin{aligned} i_{grid\_dq} = {} & i_{dq\_1}^{1+} + i_{dq\_5}^{5-} e^{-j6\omega t} + i_{dq\_7}^{7+} e^{j6\omega t} \\ & + i_{dq\_11}^{11-} e^{-j12\omega t} + i_{dq\_13}^{13+} e^{j12\omega t} \end{aligned} \quad (9)$$

Equation (6) shows that in the $dq$ synchronous rotating coordinate system, the harmonic components of voltage and current the grid side are AC variables. In the proportional resonance control of the grid side converter, in order to avoid the influence of each harmonic current on the fundamental current control, the low pass filter(LPF) is used to filter out each AC components, which can realize the effective control of the fundamental current component.

Considering that the grid-connected harmonic current is suppressed in the steady state, and the frequency of each harmonic current component is basically constant, in order to avoid the mutual influence of each harmonic current, and to simplify the design of the controller, the suppression control of each harmonic current can be realized in the multi-synchronous rotating coordinate system shown in Fig.1. In this paper, the 5th harmonic voltage equation is taken as an example. Equation (2) is transformed into 5th synchronous rotating coordinate system by constant amplitude coordinate transformation, as follows.

$$\begin{aligned} u_{grid\_dq} = {} & u_{ctrl\_dq} + R_{grid} i_{grid\_dq} \\ & + L_{grid} \frac{di_{grid\_dq}}{dt} - j5\omega L_{grid} i_{grid\_dq} \end{aligned} \quad (10)$$

In which $u_{grid\_dq}$, $u_{ctrl\_dq}$, $i_{grid\_dq}$ is as follows, respectively.

$$\begin{aligned} u_{grid\_dq} = {} & u_{dq\_1}^{1+} e^{j6\omega t} + u_{dq\_5}^{5-} + u_{dq\_7}^{7+} e^{j12\omega t} \\ & + u_{dq\_11}^{11-} e^{-j6\omega t} + u_{dq\_13}^{13+} e^{j18\omega t} \end{aligned} \quad (11)$$

$$\begin{aligned} u_{ctrl\_dq} = {} & u_{ctrl\_dq\_1}^{1+} e^{j6\omega t} + u_{ctrl\_dq\_5}^{5-} + u_{ctrl\_dq\_7}^{7+} e^{j12\omega t} \\ & + u_{ctrl\_dq\_11}^{11-} e^{-j6\omega t} + u_{ctrl\_dq\_13}^{13+} e^{j18\omega t} \end{aligned} \quad (12)$$

$$\begin{aligned} i_{grid\_dq} = {} & i_{dq\_1}^{1+} e^{j6\omega t} + i_{dq\_5}^{5-} + i_{dq\_7}^{7+} e^{j12\omega t} \\ & + i_{dq\_11}^{11-} e^{-j6\omega t} + i_{dq\_13}^{13+} e^{j18\omega t} \end{aligned} \quad (13)$$

Equation (11) to (13) show that in the 5th synchronous rotating coordinate system, only the 5th harmonic voltage and current components are DC component, while the fundamental wave and 7th, 11th, 13th harmonic components are AC component. Therefore, with the help of the low-pass filter, the AC components can be filtered out, and the 5th harmonic voltage equation of the grid-side converter is obtained, as follows.

$$\begin{aligned} u_{grid\_dq\_5} = {} & u_{ctrl\_dq\_5} + R_{grid} i_{grid\_dq\_5} \\ & + L_{grid} \frac{di_{grid\_dq\_5}}{dt} - j5\omega L_{grid} i_{grid\_dq\_5} \end{aligned} \quad (14)$$

Similarly, other order harmonic voltage equations can be obtained as follows.

$$\begin{aligned} u_{grid\_dq\_7} = {} & u_{ctrl\_dq\_7} + R_{grid} i_{grid\_dq\_7} \\ & + L_{grid} \frac{di_{grid\_dq\_7}}{dt} + j7\omega L_{grid} i_{grid\_dq\_7} \end{aligned} \quad (15)$$

$$\begin{aligned} u_{grid\_dq\_11} = {} & u_{ctrl\_dq\_11} + R_{grid} i_{grid\_dq\_11} \\ & + L_{grid} \frac{di_{grid\_dq\_11}}{dt} - j11\omega L_{grid} i_{grid\_dq\_11} \end{aligned} \quad (16)$$

$$\begin{aligned} u_{grid\_dq\_13} = {} & u_{ctrl\_dq\_13} + R_{grid} i_{grid\_dq\_13} \\ & + L_{grid} \frac{di_{grid\_dq\_13}}{dt} + j13\omega L_{grid} i_{grid\_dq\_13} \end{aligned} \quad (17)$$

## III. DESIGN OF HARMONIC CURRENT SUPPRESSION CONTROL STRATEG

### A. HARMONIC CURRENT SUPPRESSION STRATEGY

In the $dq$ multi-synchronous rotating coordinate system, from (14) to (17), the 5th, 7th, 11th and 13th harmonic voltage (18) to (21) of the grid-connected converter can be obtained, as follows:

$$\begin{cases} u_{grid\_d\_5} = u_{ctrl\_d\_5} + R_{grid} i_{grid\_d\_5} \\ \qquad + L_{grid} \dfrac{di_{grid\_d\_5}}{dt} + 5\omega L_{grid} i_{grid\_q\_5} \\ u_{grid\_q\_5} = u_{ctrl\_q\_5} + R_{grid} i_{grid\_q\_5} \\ \qquad + L_{grid} \dfrac{di_{grid\_q\_5}}{dt} - 5\omega L_{grid} i_{grid\_d\_5} \end{cases} \quad (18)$$

$$\begin{cases} u_{grid\_d\_7} = u_{ctrl\_d\_7} + R_{grid} i_{grid\_d\_7} \\ \quad + L_{grid} \dfrac{di_{grid\_d\_7}}{dt} - 7\omega L_{grid} i_{grid\_q\_7} \\ u_{grid\_q\_7} = u_{ctrl\_q\_7} + R_{grid} i_{grid\_q\_7} \\ \quad + L_{grid} \dfrac{di_{grid\_q\_7}}{dt} + 7\omega L_{grid} i_{grid\_d\_7} \end{cases} \tag{19}$$

$$\begin{cases} u_{grid\_d\_11} = u_{ctrl\_d\_11} + R_{grid} i_{grid\_d\_11} \\ \quad + L_{grid} \dfrac{di_{grid\_d\_11}}{dt} + 11\omega L_{grid} i_{grid\_q\_11} \\ u_{grid\_q\_11} = u_{ctrl\_q\_11} + R_{grid} i_{grid\_q\_11} \\ \quad + L_{grid} \dfrac{di_{grid\_q\_11}}{dt} - 11\omega L_{grid} i_{grid\_d\_11} \end{cases} \tag{20}$$

$$\begin{cases} u_{grid\_d\_13} = u_{ctrl\_d\_13} + R_{grid} i_{grid\_d\_13} \\ \quad + L_{grid} \dfrac{di_{grid\_d\_13}}{dt} - 13\omega L_{grid} i_{grid\_q\_13} \\ u_{grid\_q\_13} = u_{ctrl\_q\_13} + R_{grid} i_{grid\_q\_13} \\ \quad + L_{grid} \dfrac{di_{grid\_q\_13}}{dt} + 13\omega L_{grid} i_{grid\_d\_13} \end{cases} \tag{21}$$

In order to simplify the analysis, the influence of power-grid harmonic voltage in (18) to (21) is included in the action of controller harmonic voltage. Therefore, the dq component of each order harmonic voltage of power grid in (18) to (21) is ignored, and the harmonic voltage equation of the system in steady state can be expressed as (22) to (25) respectively.

$$\begin{cases} u_{ctrl\_d\_5} = -R_{grid} i_{grid\_d\_5} - 5\omega L_{grid} i_{grid\_q\_5} \\ u_{ctrl\_q\_5} = -R_{grid} i_{grid\_q\_5} + 5\omega L_{grid} i_{grid\_d\_5} \end{cases} \tag{22}$$

$$\begin{cases} u_{ctrl\_d\_7} = -R_{grid} i_{grid\_d\_7} + 7\omega L_{grid} i_{grid\_q\_7} \\ u_{ctrl\_q\_7} = -R_{grid} i_{grid\_q\_7} - 7\omega L_{grid} i_{grid\_d\_7} \end{cases} \tag{23}$$

$$\begin{cases} u_{ctrl\_d\_11} = -R_{grid} i_{grid\_d\_11} - 11\omega L_{grid} i_{grid\_q\_11} \\ u_{ctrl\_q\_11} = -R_{grid} i_{grid\_q\_11} + 11\omega L_{grid} i_{grid\_d\_11} \end{cases} \tag{24}$$

$$\begin{cases} u_{ctrl\_d\_13} = -R_{grid} i_{grid\_d\_13} + 13\omega L_{grid} i_{grid\_q\_13} \\ u_{ctrl\_q\_13} = -R_{grid} i_{grid\_q\_13} - 13\omega L_{grid} i_{grid\_d\_13} \end{cases} \tag{25}$$

Considering that the resistance of the grid side inlet reactor of MW class grid-connected converter is generally very small, it can be seen from (22) to (25) that the rotational voltage in each harmonic voltage equation plays a leading role. With the increase of the harmonic order, the cross-coupling effect of the rotating voltage is stronger. Therefore, when constructing the harmonic voltage controller, the cross-coupling effect of the harmonic should be considered, that is, the d-axis harmonic control voltage mainly affects the q-axis harmonic current, while the q-axis harmonic control voltage mainly affects the d-axis harmonic current.

Because the grid-side harmonic current can be suppressed in the steady state, the conventional PI regulator can still be used to realize the harmonic current suppression control. For the d-axis harmonic current control, the q-axis current can be adjusted by closed-loop PI, and the corresponding d-axis control voltage can be obtained by adding the d-axis resistance compensation term. For the q-axis harmonic current control, the d-axis current can be adjusted by closed-loop PI, and the corresponding q-axis control voltage can be obtained by adding the q-axis resistance compensation term. Combining (22) to (25), the harmonic current control (26) to (29) of the grid-side converter in multi-synchronous rotating coordinate system can be further obtained, as follows.

$$\begin{cases} u_{ctrl\_d\_5} = -R_{grid} i_{grid\_d\_5} - 5\omega L_{grid} (K_{p\_5} + \dfrac{K_{i\_5}}{s}) \\ \quad \times (i^*_{grid\_q\_5} - i_{grid\_q\_5}) \\ u_{ctrl\_q\_5} = -R_{grid} i_{grid\_q\_5} + 5\omega L_{grid} (K_{p\_5} + \dfrac{K_{i\_5}}{s}) \\ \quad \times (i^*_{grid\_d\_5} - i_{grid\_d\_5}) \end{cases} \tag{26}$$

$$\begin{cases} u_{ctrl\_d\_7} = -R_{grid} i_{grid\_d\_7} + 7\omega L_{grid} (K_{p\_7} + \dfrac{K_{i\_7}}{s}) \\ \quad \times (i^*_{grid\_q\_7} - i_{grid\_q\_7}) \\ u_{ctrl\_q\_7} = -R_{grid} i_{grid\_q\_7} - 7\omega L_{grid} (K_{p\_7} + \dfrac{K_{i\_7}}{s}) \\ \quad \times (i^*_{grid\_d\_7} - i_{grid\_d\_7}) \end{cases} \tag{27}$$

$$\begin{cases} u_{ctrl\_d\_11} = -R_{grid} i_{grid\_d\_11} - 11\omega L_{grid} (K_{p\_11} + \dfrac{K_{i\_11}}{s}) \\ \quad \times (i^*_{grid\_q\_11} - i_{grid\_q\_11}) \\ u_{ctrl\_q\_11} = -R_{grid} i_{grid\_q\_11} + 11\omega L_{grid} (K_{p\_11} + \dfrac{K_{i\_11}}{s}) \\ \quad \times (i^*_{grid\_d\_11} - i_{grid\_d\_11}) \end{cases} \tag{28}$$

$$\begin{cases} u_{ctrl\_d\_13} = -R_{grid} i_{grid\_d\_13} + 13\omega L_{grid} (K_{p\_13} + \dfrac{K_{i\_13}}{s}) \\ \quad \times (i^*_{grid\_q\_13} - i_{grid\_q\_13}) \\ u_{ctrl\_q\_13} = -R_{grid} i_{grid\_q\_13} - 13\omega L_{grid} (K_{p\_13} + \dfrac{K_{i\_13}}{s}) \\ \quad \times (i^*_{grid\_d\_13} - i_{grid\_d\_13}) \end{cases} \tag{29}$$

In which $K_{p\_k}$ and $K_{i\_k}$ are the proportion coefficient and integral coefficient of $k$-order harmonic current PI regulator, respectively.

Fig. 2. is a block diagram of grid-side converter control system with cross-coupling control. In the control system, the low pass filter is used to detect the dq axis component of the harmonic current. Because the lowest frequency of the AC current component of the dq axis is 300Hz in each rotating coordinate system, the cut-off frequency of the low-pass filter in each harmonic detection channel is 50 Hz, which can not only ensure the accurate DC component and reduce the interaction between the harmonic currents, but also make the system have better dynamic characteristics [26]–[30]. For the fundamental current control of the control system, in order to effectively filter out the harmonic current in the fundamental current and make the fundamental current have excellent dynamic regulation ability, It is necessary to ensure that the fundamental current control has a certain response bandwidth. Therefore, the cut-off frequency of the low-pass filter in the fundamental current detection channel of the system is selected to be 100Hz. The control parameters of the fundamental current are as follows: the control period of the system is 200$\mu$s, the proportional coefficient is 0.5, the inte-

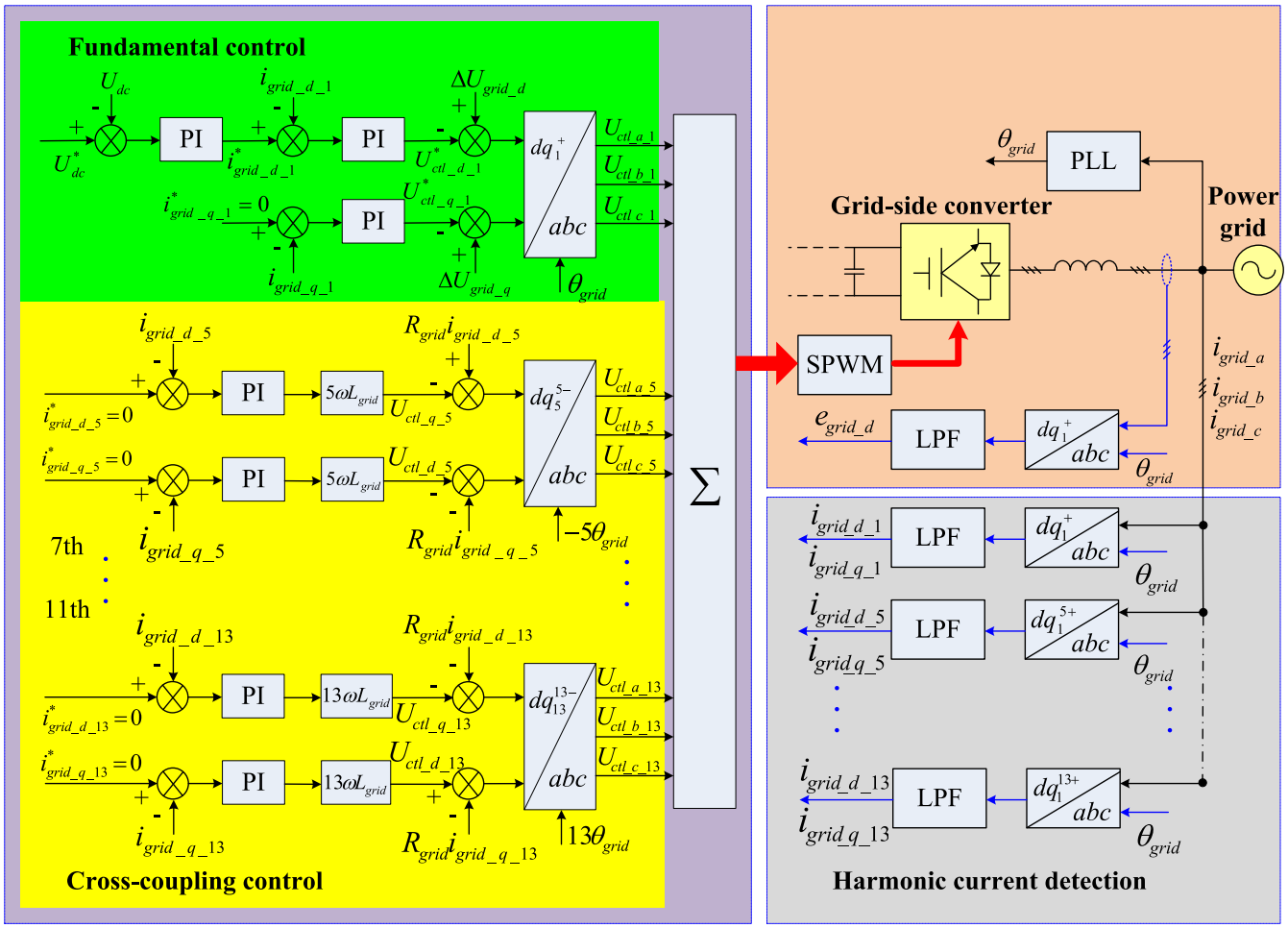


**FIGURE 2.** Control diagram of grid-side converter with cross-coupling control.

gral coefficient is 0.05, and the integral period is 10$\mu$s. In the control system, the fundamental voltage control adopts the traditional voltage and current closed-loop control mode to realize the stable control of DC chain voltage. The given value of each harmonic current is set to 0, and the corresponding harmonic current compensation voltage is generated by using each harmonic current suppression control, which is added to the fundamental control voltage to obtain the total output control voltage of the system.

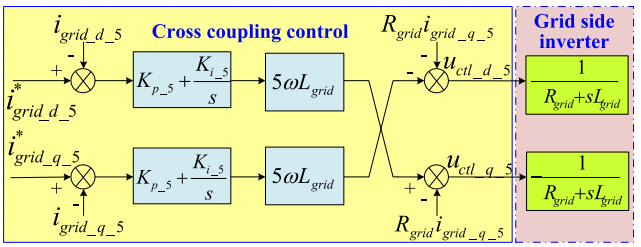


**FIGURE 3.** Control diagram of 5th harmonic current with cross-coupling control.

### B. DESIGN OF CROSS-COUPLING CONTROLLER

In this paper, the 5th harmonic current controller is taken as an example. The block diagram of the 5th harmonic current suppression control can be obtained from the mathematical model of grid side converter (26) to (29), as shown in Fig. 3.

From Fig. 3, it can be seen that when deducing the transfer function of the cross-coupling controller, the disturbance term is ignored, and when the transfer function of the d-axis control channel is obtained, the q-axis current is given to 0. While when the q-axis control channel transfer function is obtained, the d-axis current is given to 0. As a result, the open-loop transfer function of the dq axis of the 5th harmonic current PI control can be obtained, as follows.

$$G(s) = \frac{25\omega^2 L_{grid}^2 (sK_{p\_5} + K_{i\_5})}{s^2 (R_{grid} + sL_{grid})^2} \tag{30}$$

In order to realize the accurate control of harmonic current, it is necessary to design the parameters of harmonic current cross coupling controller. Considering that the phase margin and crossing frequency are related to the stability of the system, and the control system also needs to ensure a certain DC gain [31]–[35]. The parameters of the 5th harmonic current cross coupling controller are determined to be

**TABLE 1. Harmonic current controller parameters.**

| Cross-coupling controller | Proportional coefficient | Integral coefficient | Crossing frequency(rad/s) | Phase margin(°) |
|---|---|---|---|---|
| 5th harmonic | 0.043 | 0.004 | 62.5 | 35.1 |
| 7th harmonic | 0.032 | 0.012 | 62.5 | 35.0 |
| 11th harmonic | 0.020 | 0.004 | 62.5 | 34.9 |
| 13th harmonic | 0.017 | 0.005 | 62.5 | 35.1 |

**TABLE 2. Simulation parameters of permanent magnet direct drive wind power generation system.**

| Generator | Value | Grid-side converter | Value |
|---|---|---|---|
| Stator rated voltage(V) | 690 | DC-side voltage(V) | 975 |
| Stator rated current(A) | 1973 | DC-side capacitance(mF) | 20 |
| Polar numbers | 60 | Inlet reactor inductance(mH) | 0.5 |
| Rated speed(rad/s) | 2.36 | Inlet reactor resistance(mΩ) | 7 |
| Stator per phase resistance(Ω) | 0.0058 | Carrier frequency(kHz) | 5 |
| AC-DC axis inductor(mH) | 2.58 | Dead time delay(μs) | 8 |

$K_{p\_5} = 0.043, K_{i\_5} = 0.004$. According to the Bode diagram of open-loop transfer function (30), the system crossing frequency is 62.5rad/s, the phase margin is 35.1°, and DC gain is 20dB. The control system has good control accuracy and stability. Similarly, according to Fig. 2, the open-loop transfer functions of other harmonic controller parameters can be can derived. And according to the Bode diagram of open-loop transfer functions, other harmonic controller parameters can be obtained. The parameters of each harmonic current controller and frequency domain indexes are shown in Table 1.

## IV. SIMULATION AND EXPERIMENTAL VERIFICATION

### A. SIMULATION VERIFICATION AND ANALYSIS

In order to verify the correctness and effectiveness of the proposed control strategy for harmonic current suppression of grid-connected converter, a simulation model of 2MW permanent magnet direct drive wind power generation system is built in Matlab/Simulink software, and the simulation research and analysis are carried out. The system parameters are shown in Table 2.

In the simulation, the harmonic contents of the 5th, 7th, 11th and 13th voltage are 2.18%, 2.15%, 1.30% and 1.41% of the fundamental component, respectively. The grid side converter operates in the mode of unit power factor, and the output rated power is 2MW. Fig. 4 shows the comparison of power grid voltage and the output current of the grid-side converter under the proportional resonance control mode,

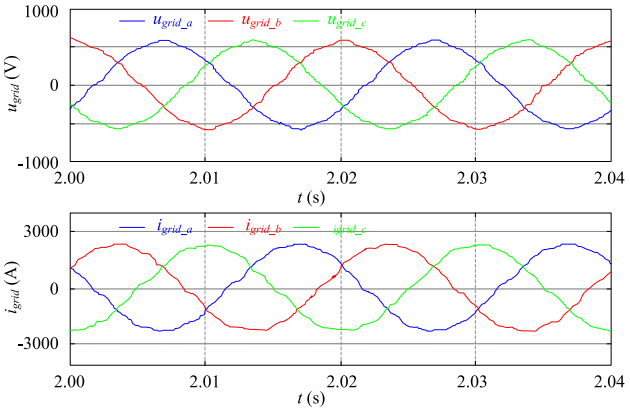


(a) Power grid voltage and the output current of the grid-side converter under proportional resonance control

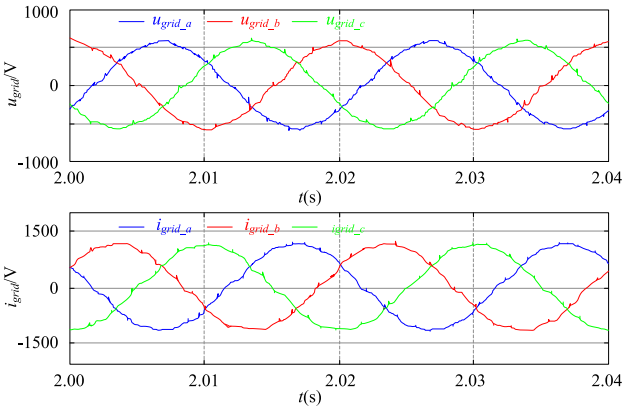


(b) Power grid voltage and the output current of the grid-side converter under proposed control without the consideration of cross-coupling effect

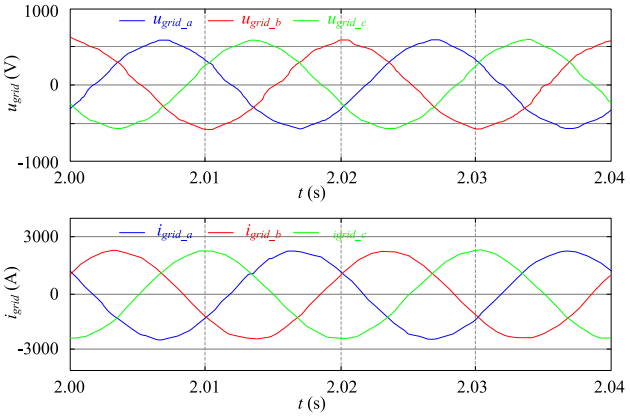


(c) Power grid voltage and the output current of the grid-side converter under cross-coupling control

**FIGURE 4. Comparison of power grid voltage and the output current of the grid-side converter under proportional resonance control, proposed control without the consideration of cross-coupling effect, cross-coupling control.**

the proposed control without the consideration of cross-coupling effect and the cross-coupling control mode when power grid voltage contains low-order harmonics. It can be seen from Fig. 4 (a) that the grid-connected current has obvious distortion and the sinusoidal degree is poor under the proportional resonance control mode. If cross-coupling effect is not considered, the proposed controller is just a

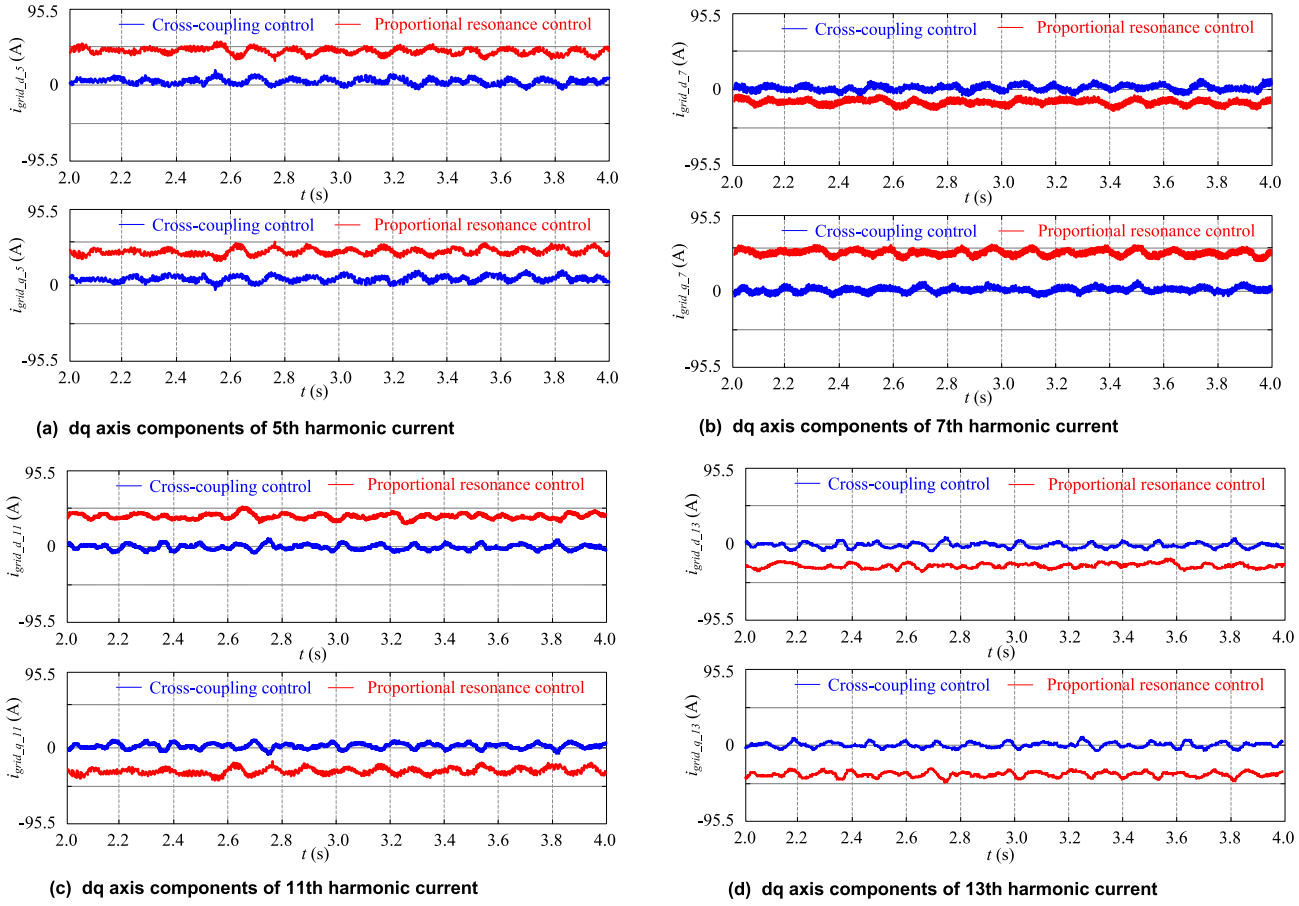


(a) dq axis components of 5th harmonic current

(b) dq axis components of 7th harmonic current

(c) dq axis components of 11th harmonic current

(d) dq axis components of 13th harmonic current

**FIGURE 5.** Comparison of dq axis components of each harmonic current between proportional resonance control and cross-coupling control.

conventional double closed-loop PI control. It can be seen from Fig. 4 (b) that the grid-connected current has serious distortion and the sinusoidal degree is more poorer than proportional resonance control under the proposed control without the consideration of cross-coupling effect. In the cross-coupling control, it can be seen from Fig. 4 (c) that the grid-connected current waveform is smooth, the distortion at the peak value is small, and the current peak burr is reduced, and the grid-connected current waveform is better.

Fig. 5 shows the comparison of the dq axis components of each harmonic current with proportional resonance control and cross-coupling control in each synchronous rotating coordinate system. From Fig. 5, it can be seen that the dq axis component of each harmonic current is large under the proportional resonance control, and the proportional resonance control strategy lacks the ability to effectively suppress the grid-connected harmonic current. While under the cross-coupling control, the low-order harmonic current components are effectively suppressed, all of which are controlled to about 0, and the harmonic current suppression control effect is good.

Fig. 6 shows the spectrum analysis of three-phase grid-connected current under proportional resonance control. From Figure.6, it can be seen that there is a high harmonic current component in the three-phase grid-connected current, and the proportion of the 5th, 7th, 11th and 13th harmonic current component in the fundamental current component is more than 1.5%. Among them, the proportion of the 5th harmonic current is up to 2%, which will lead to a serious decline in the output power quality of wind power generation system.

Fig. 7 shows the spectrum analysis of three-phase grid-connected current under cross-coupling control. It can be seen from Fig. 7 that compared with the proportional resonance control, the proportion of each low harmonic current component in the fundamental current component is greatly reduced. The proportion of the 5th, 7th, 11th and 13th harmonic current component in the fundamental current component is all controlled below 0.5%, which further proves the excellent suppression and control performance of the harmonic current cross-coupling controller to the grid-connected harmonic current.

Table 3 shows the comparison of the harmonic content of three-phase grid-connected current with proportional resonance control and cross-coupling control. Therefore, it can be seen that the output power quality of wind power generation system under cross-coupling control

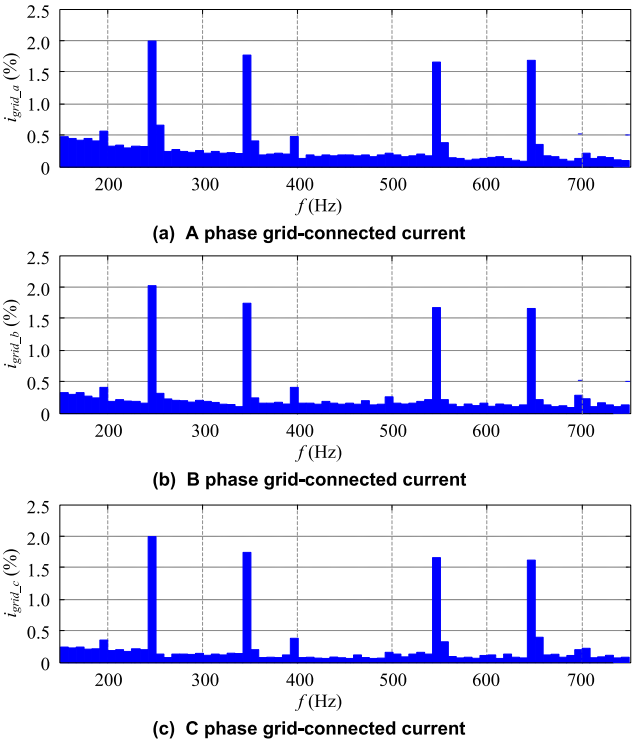


**FIGURE 6.** Frequency spectrum analysis of three-phase grid-connected current under proportional resonance control.

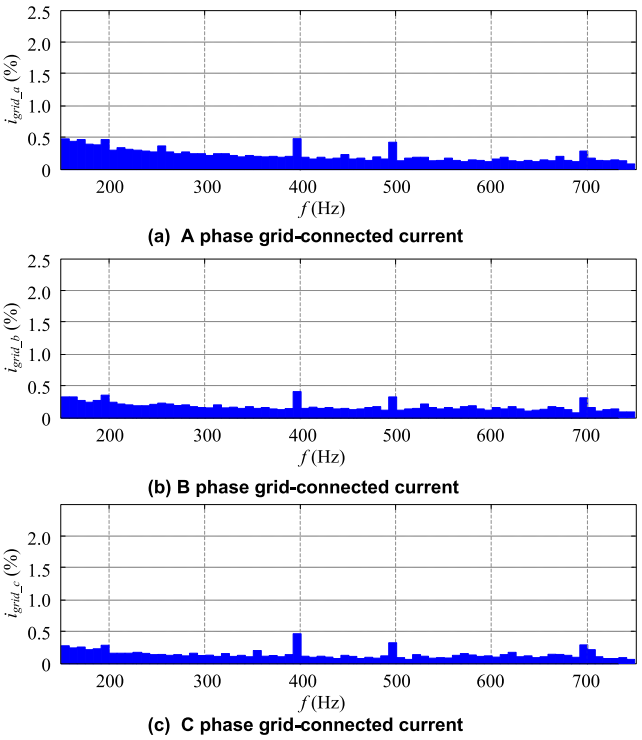


**FIGURE 7.** Frequency spectrum analysis of three-phase grid-connected current under cross-coupling control.

has been greatly improved, and the reliability of power generation system and power grid operation has also been improved.

**TABLE 3.** Comparisons of grid-connected current harmonic contents between proportional resonance control and cross-coupling control.

| Control strategy | 5th harmonic current content/% | | |
|---|---|---|---|
| | A phase | B phase | C phase |
| Proportional resonance control | 1.97 | 2.00 | 2.00 |
| Cross-coupling control | 0.30 | 0.41 | 0.44 |
| Control strategy | 7th harmonic current content/% | | |
| | A phase | B phase | C phase |
| Proportional resonance control | 1.77 | 1.72 | 1.74 |
| Cross-coupling control | 0.22 | 0.18 | 0.20 |
| Control strategy | 11th harmonic current content/% | | |
| | A phase | B phase | C phase |
| Proportional resonance control | 1.65 | 1.64 | 1.65 |
| Cross-coupling control | 0.15 | 0.16 | 0.13 |
| Control strategy | 13th harmonic current content/% | | |
| | A phase | B phase | C phase |
| Proportional resonance control | 1.66 | 1.64 | 1.62 |
| Cross-coupling control | 0.16 | 0.14 | 0.11 |

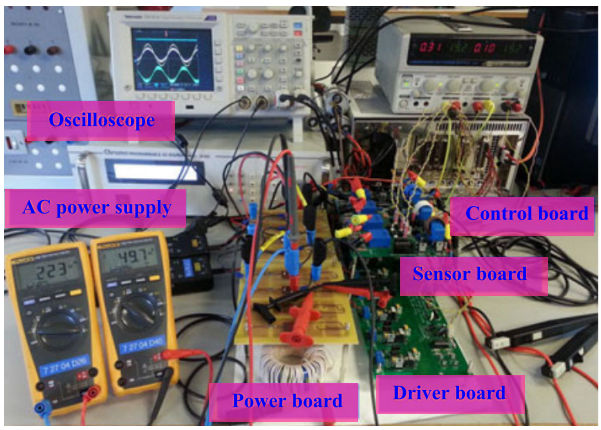


**FIGURE 8.** Experimental platform of grid-side converter.

### B. EXPERIMENTAL VERIFICATION AND ANALYSIS

In order to further verify the feasibility of the proposed control strategy, a small power grid-connected converter experimental platform is established, which test the control effect of the grid-side converter. Fig. 8 shows the experimental platform, which is mainly composed of three-phase grid-side converter, inlet reactor, three-phase isolation transformer, self-coupling voltage regulator, DC power supply and

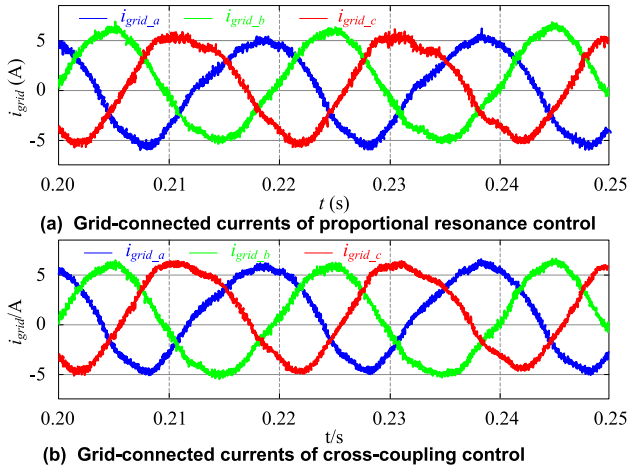


**FIGURE 9.** Experiment results between proportional resonance control and cross-coupling control.

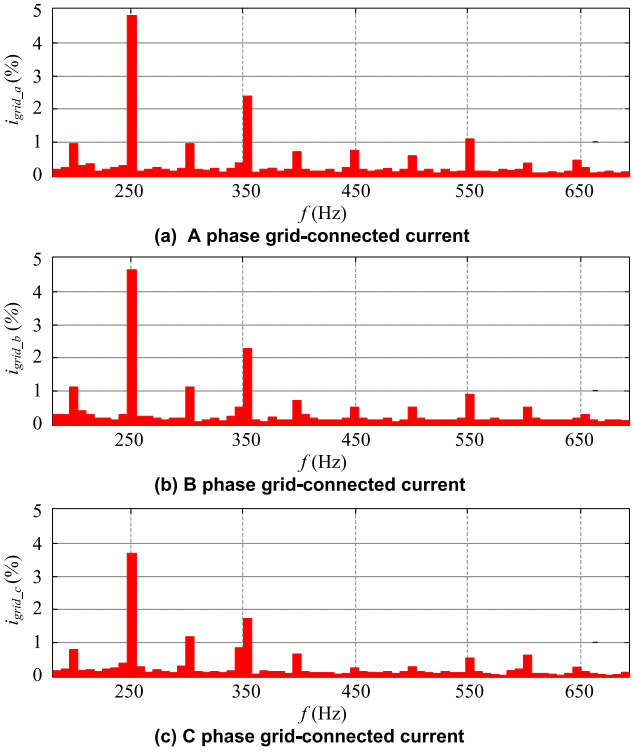


**FIGURE 10.** Frequency spectrum analysis of three-phase grid-connected current under proportional resonance control.

control system. The inlet reactor resistance $R_{grid}$ is 0.1Ω, the inlet reactor inductance $L_{grid}$ is 3mH, the DC side capacitance C is 2200$\mu$F, the DC side voltage is 100V, the switching frequency is 10kHz, and the dead time delay is 3$\mu$s. The main controller of the grid side converter control system adopts the special digital processing chip *cyclone III EP3C40Q240C8N* of Altera company, which process the voltage and current signals collected by the control system. The control algorithm proposed in this paper is used to generate pulse width modulation drive signal to control the fundamental current and harmonic current of the grid-side converter.

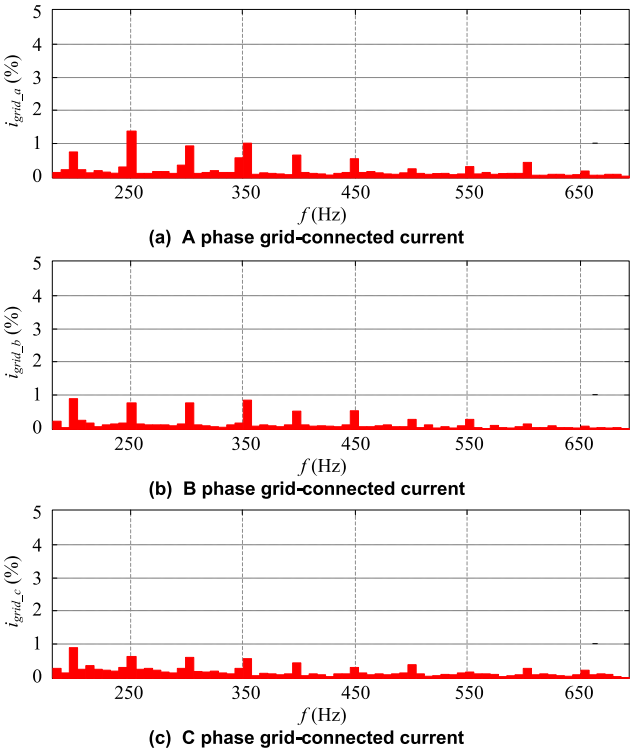


**FIGURE 11.** Frequency spectrum analysis of three-phase grid-connected current under cross-coupling control.

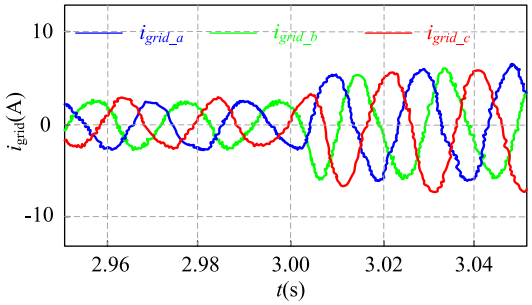


**FIGURE 12.** Grid-connected currents of step dynamic response of active power under cross-coupling control.

When the grid-side converter of the experimental platform works at the unit power factor and outputs 4A active current, the waveform of three-phase grid-connected current is shown in Fig. 9. Fig. 9(a) shows a three-phase grid-connected current waveform under proportional resonance control. Fig. 9(b) shows a three-phase grid-connected current waveform under cross-coupling control. From Fig. 9, it can be seen that there are many sharp burrs in grid-connected current under proportional resonance control, the current waveform is rough and not smooth, and the distortion at the peak value is large. While under cross-coupling control, the grid-connected current is smoother. The peak and peak distortion is small, and the burr of current peak is reduced, and the waveform of grid-connected current is better.

Fig. 10 shows the harmonic analysis diagram of three-phase grid-connected current under proportional resonance control. Fig. 11 shows the harmonic analysis diagram of three-phase grid-connected current under cross-coupling

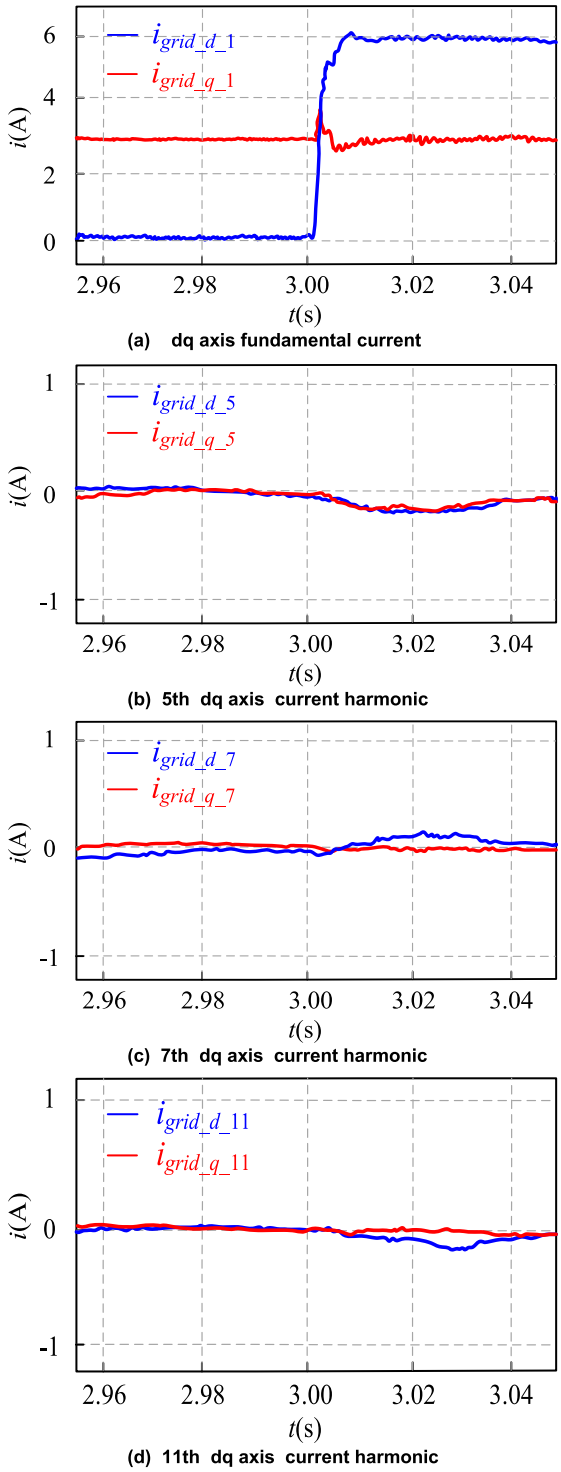


**FIGURE 13.** dq axis current component of step dynamic response of active power under cross-coupling control.

control. Compared with Fig. 10 and Fig. 11, it can be seen that when the proportional resonance control strategy is adopted, the grid-side three-phase current distortion is more serious and the sinusoidal degree is poor. The amplitude of the 5th and 7th harmonic current is relatively large. While when the cross-coupling control strategy is adopted, the sinusoidal degree of grid-side current is improved, and the proportion of low-order harmonic current is greatly reduced. Taking A phase current as an example, The proportion of the 5th harmonic current component in the fundamental current decreases from 4.993% to 1.392%, and the proportion of the 7th harmonic current component in the fundamental current decreases from 2.384% to 1.079%. Therefore, it can be seen that the control strategy proposed in this paper has a good suppression effect on the low-order harmonic current of the grid-connected converter.

In order to further verify the dynamic response performance of the proposed control strategy in this paper, active power step dynamic response experiment of the grid-side converter is carried out. Fig. 12 shows the dynamic response waveform of the three-phase grid-side current. Fig.13 shows the dq axis component waveforms of fundamental current, 5th, 7th and 11th harmonic current.

The grid-side converter runs with a unit power factor before 3s, and changes to an output active power of 420W at 3s. Fundamental active current component control is accurate and fast. At the same time, each harmonic current is suppressed to 0 after the active current step, which shows that the proposed control method can realize the fast and accurate regulation of fundamental current, and each harmonic current can be effectively suppressed. The grid-side converter has excellent current regulation performance and good dynamic response.

## V. CONCLUSION

Due to the power-grid low-order harmonic voltage and the nonlinearity of power electronic devices, the grid-connected converter of wind power generation system produces grid-connected harmonic current. In order to improve the output power quality of full-power grid-connected converter of wind power generation system, the harmonic mathematical model of grid-side converter is established in this paper. On this basis, a cross-coupling current control strategy for suppressing the low-order harmonic current components is proposed. The proposed control strategy takes into account the cross-coupling effect of each harmonic current, which can realize the accurate control of grid-connected harmonic current, and can suppress the grid-connected harmonic current caused by the power-grid low-order harmonic voltage and the nonlinear characteristics of the grid-connected converter at the same time. The correctness and feasibility of the proposed control strategy are verified by simulation and experimental test, which is of great significance to further improve the output power quality of the grid-connected full-power converter of wind power generation system. In the next step, the proposed control strategy is applied to the LCL filter inverter to verify the harmonic current suppression performance of the control strategy and the stability of the system, and compared with other control strategies.

## REFERENCES

[1] M. Reyes, P. Rodriguez, S. Vazquez, A. Luna, R. Teodorescu, and J. M. Carrasco, "Enhanced decoupled double synchronous reference frame current controller for unbalanced grid-voltage conditions," *IEEE Trans. Power Electron.*, vol. 27, no. 9, pp. 3934–3943, Sep. 2012.

[2] D. N. Zmood and D. G. Holmes, "Stationary frame current regulation of PWM inverters with zero steady-state error," *IEEE Trans. Power Electron.*, vol. 18, no. 3, pp. 814–822, May 2003.

[3] L. Quanwei, D. Yan, and H. Yihua, "Current prediction and virtual oversampling based digital hysteresis control," *Trans. China Electrotech. Soc.*, vol. 29, no. 10, pp. 127–133, 2014.

[4] M. F. M. Arani and Y. A.-R.-I. Mohamed, "Assessment and enhancement of a full-scale PMSG-based wind power generator performance under faults," *IEEE Trans. Energy Convers.*, vol. 31, no. 2, pp. 728–739, Jun. 2016.

[5] J. Yaoqin, Z. Minglin, and F. Yong, "State feedback based repetitive control for single-phase inverter," *Trans. China Electrotech. Soc.*, vol. 29, no. 6, pp. 57–63, 2014.

[6] M. Pichan, H. Rastegar, and M. Monfared, "Deadbeat control of the standalone four-leg inverter considering the effect of the neutral line inductor," *IEEE Trans. Ind. Electron.*, vol. 64, no. 4, pp. 2592–2601, Apr. 2017.

[7] W. Jiang, X. Ding, Y. Ni, J. Wang, L. Wang, and W. Ma, "An improved deadbeat control for a three-phase three-line active power filter with current-tracking error compensation," *IEEE Trans. Power Electron.*, vol. 33, no. 3, pp. 2061–2072, Mar. 2018.

[8] L. Yu, "Effects of converter pulse volage on insulation life of doubly-fed wind generators," *Power Equip.*, vol. 28, no. 3, pp. 186–188, Mar. 2014.

[9] L. Sainz, J. J. Mesas, R. Teodorescu, and P. Rodriguez, "Deterministic and stochastic study of wind farm harmonic currents," *IEEE Trans. Energy Convers.*, vol. 25, no. 4, pp. 1071–1080, Dec. 2010.

[10] Y. Jun, X. Xianfeng, C. Xiyin, and L. Yong, "Harmonic currents suppression for full size power grid-connection converter used for wind power generation," *Proc. CSEE*, vol. 32, no. 16, pp. 17–25, Jun. 2012.

[11] H. Yang, P. Li, Y. Xia, and C. Yan, "Double-loop stability for high frequency networked control systems subject to actuator saturation," *IEEE Trans. Cybern.*, vol. 49, no. 4, pp. 1454–1462, Apr. 2019.

[12] X.-H. Chang and Y.-M. Wang, "Peak-to-Peak filtering for networked nonlinear DC motor systems with quantization," *IEEE Trans Ind. Informat.*, vol. 14, no. 12, pp. 5378–5388, Dec. 2018.

[13] Z. Yang and D. Xu, "Stability analysis and design of impulsive control systems with time delay," *IEEE Trans. Autom. Control*, vol. 52, no. 8, pp. 1448–1454, Aug. 2007.

[14] L. Dong and Y. Takeuchi, "Impulsive control of multiple Lotka–Volterra systems," *Nonlinear Anal., Real World Appl.*, vol. 14, no. 2, pp. 1144–1154, Feb. 2013.

[15] X. Hailiang, H. Jiabing, and H. Yikang, "Modeling and control of wind turbine driven doubly-fed induction generators under harmonic grid voltage conditions," *Automat. Electr. Power Syst.*, vol. 35, no. 11, pp. 20–26, 2011.

[16] D. Xiang, J. C. Turu, S. M. Muratel, and T. Wang, "On-site LVRT testing method for full-power converter wind turbines," *IEEE Trans. Sustain. Energy*, vol. 8, no. 1, pp. 395–403, Jan. 2017.

[17] X. Lei, H. Shoudao, and H. Keyuan, "Harmonic suppression for the motor-side converter of the directly-driven wind turbine with PM synchronous generator," *Proc. CSEE*, vol. 31, no. 6, pp. 31–37, 2011.

[18] Y. Jun, C. Xiyin, and L. Yong, "Grid-connected control of a direct-driven permanent magnet wind power generation system with restraining the negative sequence and harmonic currents," *Power Syst. Technol.*, vol. 35, no. 7, pp. 29–35, 2011.

[19] S. Li, J. Zhang, and W. Tang, "Robust $H_\infty$ control for impulsive switched complex delayed networks," *Math. Comput. Model.*, vol. 56, nos. 11–12, pp. 257–267, Dec. 2012.

[20] H. Geng, C. Liu, and G. Yang, "LVRT capability of DFIG-based WECS under asymmetrical grid fault condition," *IEEE Trans. Ind. Electron.*, vol. 60, no. 6, pp. 2495–2509, Jun. 2013.

[21] Z. Zhang and P. Wang, "Research and implementation of natural sampling SPWM digital method for three-level inverter of photovoltaic power generation system based on FPGA," *IEEE Access*, vol. 7, pp. 114449–114458, 2019.

[22] S. Bhattacharya, D. Mascarella, and G. Joos, "Space-Vector-Based generalized discontinuous pulsewidth modulation for three-level inverters operating at lower modulation indices," *IEEE J. Emerg. Sel. Topics Power Electron.*, vol. 5, no. 2, pp. 912–924, Jun. 2017.

[23] K. Ilves, F. Taffner, S. Norrga, A. Antonopoulos, L. Harnefors, and H.-P. Nee, "A submodule implementation for parallel connection of capacitors in modular multilevel converters," *IEEE Trans. Power Electron.*, vol. 30, no. 7, pp. 3518–3527, Jul. 2015.

[24] S. Essakiappan, H. S. Krishnamoorthy, P. Enjeti, R. S. Balog, and S. Ahmed, "Multilevel medium-frequency link inverter for utility scale photovoltaic integration," *IEEE Trans. Power Electron.*, vol. 30, no. 7, pp. 3674–3684, Jul. 2015.

[25] M. Hasan, S. Mekhilef, and M. Ahmed, "Three-phase hybrid multilevel inverter with less power electronic components using space vector modulation," *IET Power Electron.*, vol. 7, no. 5, pp. 1256–1265, May 2014.

[26] A. Salem, E. M. Ahmed, M. Orabi, and M. Ahmed, "New three-phase symmetrical multilevel voltage source inverter," *IEEE J. Emerg. Sel. Topics Circuits Syst.*, vol. 5, no. 3, pp. 430–442, Sep. 2015.

[27] A. Salem, E. M. Ahmed, M. Ahmed, M. Orabi, and A. B. Abdelghani, "Reduced switches based three-phase multi-level inverter for grid integration," in *Proc. IREC 6th Int. Renew. Energy Congr.*, Mar. 2015, pp. 1–6.

[28] M. D. Siddique, S. Mekhilef, N. M. Shah, A. Sarwar, A. Iqbal, M. Tayyab, and M. K. Ansari, "Low switching frequency based asymmetrical multilevel inverter topology with reduced switch count," *IEEE Access*, vol. 7, pp. 86374–86383, 2019.

[29] H. M. Basri and S. Mekhilef, "Digital predictive current control of multilevel four-leg voltage-source inverter under balanced and unbalanced load conditions," *IET Electr. Power Appl.*, vol. 11, no. 8, pp. 1499–1508, Sep. 2017.

[30] Z. Zhang, P. Zhang, and F. Gao, "Research on synchronous control method for suppressing nonlinear impulse perturbation of photovoltaic grid-connected inverter," *IEEE Access*, vol. 8, pp. 22303–22313, 2020.

[31] W. Rui, S. Qiuye, M. Dazhong, and H. Xuguang, "Line impedance cooperative stability region identification method for grid-tied inverters under weak grids," *IEEE Trans. Smart Grid*, to be published, doi: 10.1109/TSG.2020.2970174.

[32] R. Wang, Q. Sun, D. Ma, and Z. Liu, "The small-signal stability analysis of the droop-controlled converter in electromagnetic timescale," *IEEE Trans. Sustain. Energy*, vol. 10, no. 3, pp. 1459–1469, Jul. 2019.

[33] A. Mishra, P. M. Tripathi, and K. Chatterjee, "A review of harmonic elimination techniques in grid connected doubly fed induction generator based wind energy system," *Renew. Sustain. Energy Rev.*, vol. 89, pp. 1–15, Jun. 2018.

[34] R. Zhao, Q. Li, H. Xu, Y. Wang, and J. M. Guerrero, "Harmonic current suppression strategy for grid-connected PWM converters with LCL filters," *IEEE Access*, vol. 7, pp. 16264–16273, 2019.

[35] C. Nie, Y. Wang, W. Lei, M. Chen, and Y. Zhang, "An enhanced control strategy for multiparalleled grid-connected single-phase converters with load harmonic current compensation capability," *IEEE Trans. Ind. Electron.*, vol. 65, no. 7, pp. 5623–5633, Jul. 2018.


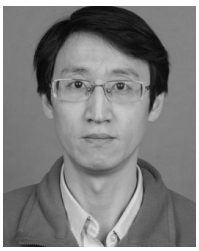

**ZHAOYAN ZHANG** received the B.S. degree in computer science and technology from the College of Mathematics and Computer Science, Hebei University, Baoding, China, in 2003, and the M.S. and Ph.D. degrees in control theory and control engineering from North China Electric Power University, Baoding, in 2011 and 2017, respectively.

From 2016 to 2018, he was a Senior Engineer with Baoding SinoSimu Technology Company, Ltd., Baoding. Since 2018, he has been an Associate Professor with the College of Electronic Information Engineering, Hebei University, where he is currently a Postdoctoral Researcher. His research interests include new energy power generation technology, power electronic converter technology, and motor speed regulation.

**PEIGUANG WANG** received the Ph.D. degree in applied mathematics from the Beijing Institute of Technology, Beijing, China, in 2000. From 2002 to 2015, he was a Visiting Professor with the Department of Mathematics and Statistics, Curtin University, Australia, many times for different durations. He is currently a Professor with the College of Electronic Information Engineering, Hebei University, China. His research interests include nonlinear analysis and numerical simulation.